Density of turbulence-induced phase dislocations

Valerii V. Voitsekhovich, Dmitri Kouznetsov, and Dmitri Kh. Morozov

Under certain conditions, light-wave propagation through turbulent media causes a specific type of phase distortion: so-called phase dislocations. A salient feature of phase dislocations is an appearance of zones where the phase turns out to be a multivalued function of coordinates. The problem of turbulence-induced phase dislocations is considered. Both a theoretical treatment and simulations based on the numerical solution of a parabolic equation are used for estimation of the dislocation density. Various turbulence conditions, ranging from weak to very strong ones, are considered as well as the dependences on wavelength, and the inner scales of turbulence are presented. An empirical formula for the dislocation density suitable for a wide range of turbulent and propagation conditions is derived. The results obtained can be useful for both atmospheric and adaptive optics.

OCIS codes: 010.1080, 010.1290, 010.1300, 010.1330, 030.7060, 030.6600.

1. Introduction

A conventional type of phase distortion, in which a phase appears to be a single-valued function of coordinates, has been investigated for a long time. However, there is another possible type of phase distortion with singularities of the phase S (so-called phase dislocations). A conception of these singularities was initially introduced into optics by Nye and Berry[1] in the middle 1970's. Since that time, many theoretical and experimental investigations supporting this conception have been published.[2–16] A salient feature of the phase dislocations is an appearance of such points where the field of the gradient S becomes a vortex one (curl grad $S \neq 0$). A necessary condition of vortex creation at some observation point is an occurrence of zero amplitude A at this point.

Various applications of phase dislocations in different areas have been suggested. Among them, the problem of turbulence-induced phase dislocations has recently attracted the growing attention of researchers working in atmospheric and adaptive optics.[17–22] Propagating in a turbulent media, a light wave passes through refractive-index inhomogeneities that cause amplitude and phase fluctuations in the observation zone. If these fluctuations turn out to be strong enough, zero-amplitude points may be produced in the observation zone, which leads to the creation of phase dislocations.

The existence of turbulence-induced dislocations was initially proved by Fried and Vaughn.[17] They carried out a numerical experiment for a laser beam propagating through Kolmogorov turbulence and presented a number of samples in which the dislocations are clearly seen. Fried and Vaughn also suggested a procedure of phase reconstruction in the presence of dislocations, which is important for applications. This last problem was later discussed by Tartakovski and Mayer,[19] who also analyzed some properties of the point-spread function associated with the dislocated phase.[22] An effect of dislocations on the performances of adaptive systems was investigated by Lukin and Fortes,[18,20] while some theoretical aspects dealing with the propagation of the dislocated phase were considered by Aksenov *et al*.[21]

Our main aim in this paper is to study the density of turbulence-induced phase dislocations as a function of the turbulence and the propagation conditions. The density of dislocations is among their most important properties. This quantity shows an expected number of dislocations to be found inside the unit area. A suitable approach allowing for the theoretical calculation of this characteristic for the case of fully developed Gaussian fields has been suggested in Ref. 4. However, the statistics of turbulence-induced distortions approach the Gaussian ones only

The authors are with Universidad Nacional Autonoma de Mexico, 04510 Distrito Federal, Mexico: V. V. Voitsekhovich is with the Instituto de Astronomia, Apartado Postal 70-264 Ciudad Universitaria; D. Kouznetsov is with the Centro de Instrumentos, Apartado Postal 70-186 Ciudad Universitaria; and D. Kh. Morozov is with the Instituto de Ciencias Nucleares, Apartado Postal 70-543 Ciudad Universitaria.

Received 14 October 1997; revised manuscript received 4 February 1998.

0003-6935/98/214525-11$15.00/0

in the limiting case of very strong turbulence whereas under other conditions these statistics take different, non-Gaussian forms.[23] Along with this, these last conditions are of main interest in many practical applications. Unfortunately, the method developed in Ref. 4 turns out to be difficult for calculations of dislocation density associated with non-Gaussian distributions. It happens because in order to apply it one needs to know a six-dimensional joint probability density function (PDF) of a two-dimensional complex field and its gradients. For the case of Gaussian distortions, this PDF is easily calculated, giving one the possibility of expressing the dislocation density analytically. However, when the field statistics are non-Gaussian, a problem of the associated PDF derivation becomes quite nontrivial.

Here we apply two other methods for calculation of the dislocation density that are more suitable for non-Gaussian fields. The first is based on a modification of the so-called level-crossing approach, which is known from the theory of random processes.[24] Although the two-dimensional level-crossing problem is generally complicated, an approach developed for treatment of this problem is applicable in our case because of the isotropy of the field fluctuations.

The second method is based on computer simulation. The simulations are performed by means of numerical solution of the parabolic equation.[25] Three-dimensional (3-D) refractive-index fluctuations are assumed to be Gaussian, and our method of simulation is similar to that used in Ref. 26. The final results for the dislocation density obtained by means of our two methods are in good agreement.

We review some general properties of dislocations in Section 2. In Section 3, the general expression for dislocation density associated with isotropic fields is derived. It is shown that the density of interest can be expressed through the PDF of the log-amplitude derivative. Section 4 presents the theoretical calculations of dislocation density for different turbulence conditions, ranging from weak to very strong. Some interesting theoretical and experimental possibilities based on our considerations are also discussed in this section. In Section 5 we describe the simulation results and compare them with the theoretical ones. In Section 6 we present a summary of our results.

2. Dislocation Structure

We now introduce two terminological definitions that are used throughout the paper. A screw-type phase singularity that occurs around an isolated zero-amplitude point is referred to as a single vortex. However, the zero-amplitude points appear in pairs and the nearest-neighbor vortices arising around these points have the opposite topological charges.[9] So the resulting phase singularity appears as a superposition of two single oppositely charged vortices separated by some distance. Below we refer to this singularity as a phase dislocation.

It has been shown[1] that the single vortex is associated with the isolated zero amplitude. If one traces the zero-amplitude point around a closed circuit, the phase increases on $2\pi n$ with each trace, where $n = \pm 1$ is the topological charge or the order of the vortex (we exclude from present considerations the high-order vortices $n = \pm 2, \pm 3, \pm 4, \ldots$, which have vanishingly small probability[12]). By convention, a vortex has a positive (negative) charge if the phase increases (decreases) on 2π with each complete counterclockwise tracking around the vortex center. So an occurrence of a zero-amplitude point forces a phase to be a non-single-valued function of coordinates. Mathematically, one can arrive at this conclusion from the following consideration.[4]

Let us consider some scalar 3-D complex wave field $E(z, \boldsymbol{\rho}) = E_1(z, \boldsymbol{\rho}) + iE_2(z, \boldsymbol{\rho})$, where z denotes the longitude coordinate and $\boldsymbol{\rho} = \{x, y\}$ is the transverse position vector. The complex envelope of this field can be expressed as

$$\begin{aligned} E(z, \boldsymbol{\rho}) &= A(z, \boldsymbol{\rho}) \exp[iS(z, \boldsymbol{\rho})], \\ A(z, \boldsymbol{\rho}) &= [E_1^2(z, \boldsymbol{\rho}) + E_2^2(z, \boldsymbol{\rho})]^{1/2}, \\ S(z, \boldsymbol{\rho}) &= \text{const.} + \text{atan2}[E_2(z, \boldsymbol{\rho}), E_1(z, \boldsymbol{\rho})], \end{aligned} \quad (1)$$

where A and S denote the amplitude and the phase of the field, respectively. The function atan2(y, x) occurring in Eq. (1) returns the arctangent of y/x in the range from $-\pi$ to π, and it is used to resolve 2π ambiguity.

Let us consider some plane at $z =$ constant. Suppose that the zero amplitude occurs in this plane at the point $\boldsymbol{\rho} = 0$. Expanding E_1 and E_2 in the vicinity of this point and keeping the linear terms only, one can get

$$\begin{aligned} S(\boldsymbol{\rho}) &= \text{atan2}(E_{20} + E_{2x}x + E_{2y}y, E_{10} + E_{1x}x + E_{1y}y), \\ \boldsymbol{\rho} &= (x, y), \end{aligned} \quad (2)$$

where the quantities E_{10}, E_{20}, E_{1x}, E_{2x}, E_{1y}, and E_{2y} are taken at $\boldsymbol{\rho} = 0$. E_{1x}, E_{2x}, E_{1y}, and E_{2y} denote the corresponding first partial derivatives of the field.

Because $A(0) = 0$, the quantities E_{10} and E_{20} in Eq. (2) are zero valued. So the lines along which the first and the second arguments of atan2 in Eq. (2) are equal to zero (in what follows, the zero lines) are the straight lines intercepting one another at the origin. If we trace the point $\boldsymbol{\rho} = 0$ around any closed circuit, we meet the zero lines of the first and the second arguments twice. As a result, when we return to the starting point of the circuit, the phase increases on 2π. So Eq. (2) describes a single vortex in linear approximation (single linear vortex) when the phase is a multivalued function of coordinates. As an illustration, let us consider a particular example of a single linear vortex. In the simplest case, when $E_{1x} = E_{2y}$ and $E_{2x} = E_{1y} = 0$, Eq. (2) is reduced to

$$S(x, y) = \text{atan2}(y, x). \quad (3)$$

Equation (3) describes a 3-D screw surface, which is shown in Fig. 1(a). This vortex has a positive topological charge because the phase increases on $+2\pi$ with each complete counterclockwise tracking around the vortex center. The above example shows

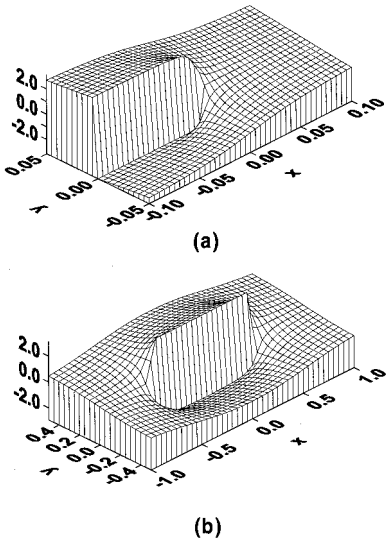

Fig. 1. Examples of (a) single linear vortex and (b) phase dislocation.

the single linear vortex that occurs if the amplitude has an isolated zero point. However, as follows from general topological considerations, the zero-amplitude points appear in pairs.[1] Moreover, the vortices arising around these points have the opposite topological charges. Hence the resulting phase turns out to be a superposition of two separated oppositely charged single vortices. The simplest example of such a dislocation can be described by the following expression [the corresponding surface is plotted in Fig. 1(b) for $x_0 = 0.5$]:

$$S(x, y) = \text{atan2}(y, x - x_0) + \text{atan2}(y, x + x_0). \quad (4)$$

As one can see from Eq. (4), this dislocation is a superposition of two oppositely charged vortices of the type shown in Fig. 1(a) that occurs at points $(-x_0, 0)$ and $(x_0, 0)$.

Comparing Figs. 1(a) and 1(b), one can see a principal difference between a single vortex and a dislocation. If one applies a single-vortex conception for the description of phase singularities in the entire space, it necessarily leads to the existence of infinitely sized phase singularities. Contrary to this, a dislocation produced by two oppositely charged vortices is a singularity that exists only between the centers of these vortices (more accurately, a singularity occurs along a line connecting the vortex centers). So a single vortex can be considered as an abstraction that is convenient for calculations, whereas a phase dislocation presents a more realistic conception for the description of physical phenomena that deal with phase singularities.

In conclusion of this section we note an important feature of dislocations. If a wave propagation is described by a linear differential equation, the field E is always a continuous, single-valued function of coordinates. Hence any phase dislocation associated with this field holds one general property: the phase jump must be equal to $2\pi n$, where n is an integer.

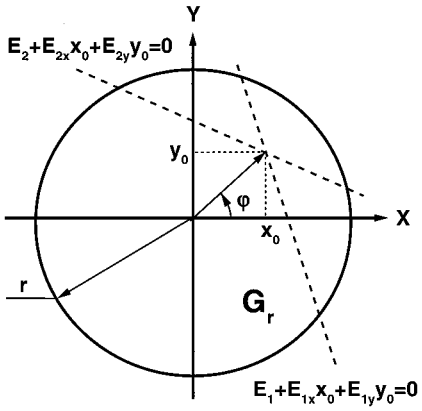

Fig. 2. Notation used for the calculations.

3. Density of the Turbulence-Induced Dislocations: Theoretical Treatment

To estimate the dislocation density λ_d it is sufficient to get a density λ_0 of amplitude zeros.[4] Since each dislocation is produced by two single vortices, there is an obvious relation: $\lambda_d = \lambda_0/2$. However, if one calculates directly the probability of zero-amplitude appearance at a given point, it turns out to be equal to zero because the event of zero amplitude has a different measure compared with the measure of the set of all possible events. For this reason a probability of zero-amplitude appearance has sense only with respect to some sized zone. The problem above is known in the theory of random processes as a level-crossing problem.[24] In our case this problem can be set up as follows.

Let $E(\boldsymbol{\rho}) = E_1(\boldsymbol{\rho}) + iE_2(\boldsymbol{\rho})$ be the two-dimensional complex wave field at the aperture. Then let us choose a small circular zone G_r of radius r (Fig. 2) inside the aperture and let $P_0(G_r)$ be a probability that zero amplitude occurs inside G_r (we choose r to be so small that no more than one zero amplitude may appear inside G_r). Since the turbulence-induced fluctuations are assumed to be statistically homogeneous, P_0 does not depend on the position of G_r at the aperture, so this position can be chosen arbitrarily. Using the notations above, we can express the density λ_0 as

$$\lambda_0 = \lim_{r \to 0} \frac{P_0(G_r)}{\pi r^2}. \quad (5)$$

Let us introduce the Cartesian coordinate system $\{x, y\}$ whose origin is at the center of zone G_r and expand the real E_1 and the imaginary E_2 parts of the field in a two-dimensional Taylor series in the vicinity of the origin. Since the magnitude of r can be chosen arbitrarily small because of the presence of the limit in Eq. (5), we can restrict the expansion by linear terms:

$$E_1(x, y) = E_{10} + E_{1x}x + E_{1y}y,$$
$$E_2(x, y) = E_{20} + E_{2x}x + E_{2y}y, \quad (6)$$

where all the quantities on the right-hand side are assumed to be taken at the origin and the quantities E_{1x}, E_{2x}, E_{1y}, and E_{2y} denote the corresponding partial derivatives of the field.

Zero amplitude occurs at the point (x_0, y_0), where both E_1 and E_2 are equal to zero. In the linear approximation [Eqs. (6)] this point is an interception point of two straight lines (Fig. 2) and its coordinates are determined from the linear system of algebraic equations:

$$E_{10} + E_{1x}x_0 + E_{1y}y_0 = 0,$$
$$E_{20} + E_{2x}x_0 + E_{2y}y_0 = 0. \tag{7}$$

Solving the system of Eqs. (7) we get

$$x_0 = -\frac{E_{10}E_{2y} - E_{20}E_{1y}}{E_{1x}E_{2y} - E_{1y}E_{2x}}, \qquad y_0 = \frac{E_{10}E_{2x} - E_{20}E_{1x}}{E_{1x}E_{2y} - E_{1y}E_{2x}}. \tag{8}$$

Introducing amplitude A, phase S, and log amplitude χ as

$$E_1 = A\cos S, \quad E_2 = A\sin S, \quad \chi = \ln(A/A_0), \tag{9}$$

where A_0 is the amplitude of the initial nondistorted wave, we can rewrite Eqs. (8) as

$$x_0 = -\frac{S_y}{\chi_x S_y - \chi_y S_x}, \qquad y_0 = \frac{S_x}{\chi_x S_y - \chi_y S_x}, \tag{10}$$

where χ_x and χ_y and S_x and S_y denote the partial derivatives of the log amplitude and the phase, respectively, taken at the origin.

In general the probability P_0 is a function of both coordinates x_0 and y_0 of the interception point. However, the turbulence-induced fluctuations are assumed to be isotropic. Under this condition the probability of interest does not depend on the polar angle φ of the interception point (Fig. 2). Hence one can choose this angle arbitrarily for the following calculations. As follows from Eqs. (10), the angle φ is expressed as

$$\tan\varphi = -S_x/S_y. \tag{11}$$

Choosing $\tan\varphi = 0$, from Eqs. (10) and (11) we get

$$x_0 = -(1/\chi_x), \qquad y_0 = 0. \tag{12}$$

As follows from Eq. (12), the probability P_0 is equal to the probability for x_0 to be inside the interval $[-r, r]$. So P_0 turns out to be a function only of x_0 because of the isotropy of the fluctuations. For the same reason P_0 is an even function of x_0, i.e., $P_0(x_0) = P_0(-x_0)$. On the other hand, Eq. (12) expresses x_0 in terms of the log-amplitude derivative χ_x taken at the origin. So, taking into account the above considerations and applying Eq. (12), we can express P_0 through the first-order PDF of the log-amplitude derivative as

$$P_0(G_r) = 2\int_{1/r}^{\infty} \mathrm{d}\chi_x W_{\chi_x}(\chi_x), \tag{13}$$

where W_{χ_x} denotes the PDF of the log-amplitude derivative. Using Eqs. (5) and (13) and recalling that $\lambda_d = \lambda_0/2$, one can get the following final expression for the dislocation density λ_d:

$$\lambda_d = \lim_{r\to 0}\frac{1}{\pi r^2}\int_{1/r}^{\infty} \mathrm{d}\chi_x W_{\chi_x}(\chi_x). \tag{14}$$

Equation (14) presents the main result of this section. As follows from Eq. (14), only the PDF of the log-amplitude derivative is necessary to calculate the dislocation density. One can see the advantages of this formula by comparing it with Eq. (18) from Ref. 4, for which one needs to know the six-dimensional PDF of the complex field and its gradient to calculate the same quantity.

Let us turn our attention to the physics of the result above. In general, the dislocation density has to depend on both amplitude and phase statistics. However, as soon as we, following Ref. 4, assume that the phase vortex arises around each zero-amplitude point, the phase statistics can be excluded from future mathematical considerations. Under this condition the dislocation density has to be a function of the amplitude statistics only. Then the level-crossing approach allows us to linearize the problem, which makes it possible to express the dislocation density as a function of the statistics of the amplitude and its first partial derivatives. Furthermore, by introducing the log amplitude, we exclude the amplitude statistics from consideration, keeping only the statistics of its partial derivatives. And finally, assuming the isotropy of fluctuations, we get Eq. (14), which includes only the PDF of one partial derivative of the log amplitude.

4. Dislocation Density for Different Turbulence Conditions

In this section we apply Eq. (14) to calculate the dislocation density from weak to very strong turbulence conditions. The turbulence conditions are usually separated by regions that are distinguished from each other by the magnitude of the so-called scintillation index β_R^2, calculated in a Rytov approximation[25] as

$$\beta_R^2 = \langle I^2\rangle/\langle I\rangle^2 - 1$$
$$= 8.7C_n^2k^2L\kappa_m^{-5/3}\left\{-1 + \frac{6}{11}D^{5/6}\left(1+\frac{1}{D^2}\right)^{11/12} \times \sin\left[\frac{11}{6}\arctan(D)\right]\right\},$$
$$D = \frac{L\kappa_m^2}{k}, \qquad \kappa_m = \frac{5.92}{l_0}, \tag{15}$$

where I denotes the intensity, C_n^2 is the structure constant, k is the wave number, L denotes the propagation length, and l_0 is the inner scale of turbulence. The quantity D, called the wave parameter, is a universal dimensionless parameter that characterizes a

wave propagation through a turbulent media with a finite inner scale. Physically it can be considered as a scaling factor between the Fresnel zone and the inner scale of turbulence.

Equations (15) follow directly from the general expression for the log-amplitude correlation function that can be found in Ref. 25, Chap. 3. The following simplified formula for the scintillation index is commonly used:

$$\beta_R{}^2 = 1.23 C_n{}^2 k^{7/6} L^{11/6}. \tag{16}$$

Equation (15) is reduced to Eq. (16) when $D \gg 1$.

The turbulence conditions are usually referred to as weak turbulence when $\beta_R{}^2 \lesssim 0.3$–1. It is assumed that the Rytov solution is valid under these conditions and that the statistics of the log amplitude are Gaussian. In the opposite limiting case, when $\beta_R{}^2$ tends to infinity, the amplitude distribution approaches the Rayleigh one,[27] which means that the statistics of field fluctuations are Gaussian. In this case the dislocation density coincides with that obtained for fully developed Gaussian fields.[4] Under intermediate conditions, which are usually referred to as strong turbulence, the statistics of amplitude are neither log normal nor Rayleigh.[27] The more popular PDF model for strong-turbulence conditions is the so-called K distribution[28] and its various modifications.

First let us estimate the dislocation density for the case of very strong turbulence that allows us to compare the final result with that obtained in Ref. 4. In the general case, the PDF of the log-amplitude derivative occurring in Eq. (14) can be expressed as

$$W_{\chi_x}(\chi_x) = \int_0^\infty \mathrm{d}A \int \mathrm{d}A_x W_2(A, A_x) \delta\left(\chi_x - \frac{A_x}{A}\right) = \int_0^\infty \mathrm{d}A A W_2(A, A\chi_x), \tag{17}$$

where W_2 is the joint PDF of the amplitude and its derivative and δ denotes the Dirac delta function.

In the case of Gaussian statistics, W_2 is a product of the Rayleigh and the Gaussian PDF's:

$$W_2(A, A_x) = \frac{1}{\sqrt{2\pi}\langle I\rangle \sigma_{A_x}} A \exp\left(-\frac{A^2}{2\langle I\rangle} - \frac{A_x{}^2}{2\sigma_{A_x}{}^2}\right), \tag{18}$$

where $\sigma_{A_x}{}^2$ is the variance of the amplitude derivative. Substituting Eq. (18) into Eq. (17), we can express W_{χ_x} as

$$W_{\chi_x}(\chi_x) = \frac{\sigma_{A_x}{}^2}{\langle I\rangle}\left(\chi_x{}^2 + \frac{\sigma_{A_x}{}^2}{\langle I\rangle}\right)^{-3/2.} \tag{19}$$

Using Eqs. (14) and (19), we have the following expression for λ_d in the case of Gaussian field statistics:

$$\lambda_d = \frac{1}{2\pi}\frac{\sigma_{A_x}{}^2}{\langle I\rangle}. \tag{20}$$

Equation (20) for λ_d coincides with that from Eq. (18) of Ref. 4.

We now turn our attention to the case of weak-turbulence conditions. It is usually assumed that under these conditions the log-amplitude fluctuations obey the Gaussian statistics. So we can write W_{χ_x} as

$$W_{\chi_x}(\chi_x) = \frac{1}{\sqrt{2\pi}\sigma_{\chi_x}} \exp\left(-\frac{\chi_x{}^2}{2\sigma_{\chi_x}{}^2}\right), \tag{21}$$

where $\sigma_{\chi_x}{}^2$ is the variance of the log-amplitude derivative. Substituting Eq. (21) into Eq. (14) and evaluating the integral, we get

$$\lambda_d = \lim_{r\to 0} \frac{1}{2\pi r^2}\left[1 - \mathrm{erf}\left(\frac{1}{\sqrt{2}\sigma_{\chi_x} r}\right)\right], \tag{22}$$

where erf denotes the error function (Ref. 29, p. 792).

Applying the asymptotic expansion of the error function, one can conclude that the limit in Eq. (22) is equal to zero. This means that dislocations never appear while the log-amplitude statistics are assumed to be Gaussian. But it does not mean that the dislocations do not occur under the weak-turbulence conditions. The Gaussian log-amplitude statistics follow from the Rytov approximate solution of parabolic equation. Hence these statistics are only an approximation of the real ones. So one may expect that, under the weak-turbulence conditions, the real statistics may deviate a little from Gaussian ones. An abundance of physical quantities that are of interest in applications are practically insensitive to such small deviations. However, dislocation density is an exception. As follows from Eq. (14), its magnitude depends strongly on the asymptotic behavior of the PDF of the log-amplitude derivative. For this reason the small asymptotic deviations of this PDF from Gaussian form can strongly affect the dislocation density. As a result, a real dislocation density under the weak-turbulence conditions may be low, but not exactly equal to zero. We continue this discussion in Section 5, which is based on the simulation results.

Let us consider now a case of strong turbulence, assuming the K distribution for amplitude fluctuations. We also assume that the PDF of the amplitude derivative is Gaussian. This assumption can be supported by the following considerations. The dislocation density is affected strongly by high-magnitude derivatives of amplitude. From the physical point of view, the main contribution to these derivatives comes from a vast number of small refractive-index inhomogeneities situated in different parts of turbulent media. So, according to the central limit theorem, we can expect Gaussian statistics for high-magnitude amplitude derivatives that are of main interest for our consideration. For simplicity we also assume that the fluctuations of amplitude and its derivative are statistically independent. Taking into account the consideration above we can

write the joint PDF of the amplitude and its derivative as a product of K and Gaussian distributions:

$$W_2(A, A_x) = \frac{4\langle I\rangle^{-(\alpha+1)/2}\alpha^{(\alpha+1)/2}}{\sigma_{A_x}\sqrt{2\pi}\Gamma(\alpha)} \times A^{\alpha}K_{\alpha-1}(2\sqrt{\alpha\langle I\rangle}A)\exp\left(-\frac{A_x^2}{2\sigma_{A_x}^2}\right), \quad (23)$$

where Γ is the gamma function and K_ν denotes the MacDonald function (modified Bessel function of the third kind, Ref. 29, p. 794). The parameter α is expressed through the scintillation index β as

$$\alpha = \frac{2}{\beta^2 - 1}, \qquad \beta^2 > 1.$$

Substituting Eq. (23) into Eq. (17), we can express the PDF W_{χ_x} as

$$W_{\chi_x}(\chi_x) = \frac{2^{(\alpha-2)/2}\langle I\rangle^{-\alpha/2}\sigma_{A_x}{}^{\alpha}\alpha^{\alpha/2}\Gamma(\alpha + 1/2)}{\Gamma(\alpha)}|\chi_x|^{-\alpha-1} \times \exp\left(\frac{\alpha\sigma_{A_x}{}^2}{\chi_x{}^2\langle I\rangle}\right)W_{-(\alpha+1)/2,(\alpha-1)/2}\left(\frac{2\alpha\sigma_{A_x}{}^2}{\chi_x{}^2\langle I\rangle}\right), \quad (24)$$

where $W_{\mu,\eta}$ denotes the Whittaker function (Ref. 29, p. 797). Substituting Eq. (24) into Eq. (14), evaluating the integral (see Ref. 29, p. 40, for details), and calculating the limit, one gets the following expression for the dislocation density:

$$\lambda_d = \frac{\sigma_{A_x}{}^2}{\pi(3 - \beta^2)\langle I\rangle}, \qquad 1 < \beta^2 < 3. \quad (25)$$

The above calculation with the K distribution gives only a rough estimate of the associated dislocation density because of the assumptions that have been made through the derivation of the joint PDF W_2 given by Eq. (23). These calculations have been made mainly for illustrative purposes to show how a criterion of dislocation appearance can be used for testing the strong-turbulence PDF's. As is shown in Section 5, the dislocations always appear under the strong-turbulence conditions. However, the K distribution is only one among the candidates for the strong-turbulence PDF; several other distributions have been suggested by different authors. Each can be tested on the existence of the limit in Eq. (16); if this limit turns out to be zero or infinity, the corresponding distribution is not a good candidate for the strong-turbulence PDF. Moreover, since a class of distributions satisfying the above criterion is not so wide, a range of searching for new PDF candidates can be narrowed at the very start.

Let us discuss another opportunity that may be interesting from both the experimental and the theoretical points of view. The results above show that the dislocations do not appear while the log-amplitude fluctuations obey Gaussian statistics. This conclusion can be used in experimental investigations to estimate the upper boundary of the region where the Gaussian statistics is applicable to the log-amplitude fluctuations. In this case an appearance of dislocations can be used as a trigger test: As soon as they occur, the statistics of the log amplitude have to be different from Gaussian.

The expressions above allow for a theoretical estimation of dislocation density but they are applicable for separate regions of turbulence conditions. Along with this, it would be interesting in applications to get a continuous approximate expression to be suitable for various turbulence conditions. We derive below such an empirical formula based on some physical considerations and our simulation results.

At first let us consider the conditions under which the dislocations just start to appear. These conditions arise as soon as the statistics of the log-amplitude derivative begin to be different from Gaussian. So we can expect that the desired expression for the dislocation density has a functional form similar to that of Eq. (22), which we obtained by using the linear expansion of the wave field inside a circular zone with radius r and by treating the case when r tends to zero. However, we can introduce a dislocation density in some other way, namely, we can consider a case when r tends to some finite value, say r_c, rather than to zero. From a mathematical viewpoint this means that the linear approximation of the wave field has to be valid inside the zone with radius r_c. From a physical viewpoint r_c can be considered as some quantity that is proportional to the correlation length of log-amplitude fluctuations. Taking into account the consideration above, we seek the expression of interest as

$$\lambda_d = \eta\left[1 - \mathrm{erf}\left(\frac{1}{\sqrt{2\sigma_{\chi_x}{}^2 r_c}}\right)\right], \quad (26)$$

where both η and r_c are some functions of the turbulence and the propagation conditions.

Taking into account the known properties of the error function, we can conclude from Eq. (26) that the conditions of interest are determined mainly by the magnitude of r_c. We hope also that the log-amplitude correlation function calculated in a Rytov approximation is still suitable under these conditions (or at least gives the correct functional dependencies). So one can use the known expression for the normalized log-amplitude correlation function b_χ to estimate r_c (Ref. 25, Chap. 3):

$$b_\chi(\rho) \approx 1 - 12.3\rho^2(\lambda L)^{-5/6}l_0{}^{-1/3} = 1 - 1.47\rho^2 D^{1/6}k/L, \quad (27)$$

where $\lambda = 2\pi/k$ is the wavelength and D is the wave parameter mentioned after Eqs. (15) above. Equating approximation (27) to zero, we get the following estimate for r_c:

$$r_c = 0.82aD^{-1/12}\sqrt{L/k},$$

where a denotes some numerical coefficient.

We now turn our attention to the function η. We assume that η in Eq. (26) is a function of the variance of the log-amplitude derivative $\sigma_{\chi_x}{}^2$ and the wave

parameter D. Hence, as follows from dimensional considerations, η is proportional to the first degree of $\sigma_{\chi_x}^2$. So we can express the function η as

$$\eta = b\sigma_{\chi_x}^2 D^{\alpha},$$

where both b and α are some numerical coefficients. Taking into account the considerations above and comparing the results with numerical simulations, we estimated the magnitudes of a, b, and α and arrived at the following empirical expression for the dislocation density:

$$\lambda_d = \frac{D^{-1/12}\sigma_{\chi_x}^2}{2\pi^2}\left[1 - \operatorname{erf}\left(\frac{\pi D^{1/12}}{4\sigma_{\chi_x}\sqrt{L/k}}\right)\right]. \quad (28)$$

As is seen in Section 5, Eq. (28) turns out to be in unexpectedly good agreement with the simulated data.

5. Simulation Results

Our simulations are based on the numerical solution of the parabolic equation that describes the propagation of monochromatic light waves through a turbulent atmosphere (Ref. 25, Chap. 2):

$$2ik\frac{\partial E(z, \boldsymbol{\rho})}{\partial z} + \Delta_{\perp}E(z, \boldsymbol{\rho}) + 2k^2\tilde{n}(z, \boldsymbol{\rho})E(z, \boldsymbol{\rho}) = 0, \quad (29)$$

where $E = E_1 + iE_2$ denotes the complex wave field, $\boldsymbol{\rho} = (x, y)$ is the transverse position vector, $\Delta_{\perp} = [(\partial^2/\partial x^2) + (\partial^2/\partial y^2)]$, $k = 2\pi/\lambda$ is the wave number, and $\tilde{n}$ denotes the refractive-index fluctuations.

Our method of simulations is practically the same as that presented in Ref. 26, so we do not describe it here; instead we refer the reader to this reference for details. Here we restrict our attention to the initial monochromatic plane wave that propagates through the turbulent atmosphere with constant parameters along the propagation path. The refractive-index fluctuations are assumed to be an isotropic Gaussian field with the corresponding spectrum Φ_n given by[25]

$$\Phi_n(\kappa) = 0.033C_n^2\kappa^{-11/3}\exp(-\kappa^2/\kappa_m^2),$$
$$\kappa_m = (5.92/l_0), \quad (30)$$

where l_0 denotes the inner scale of the turbulence.

Although there are other, more advanced inner-scale models, we have applied the simplest one above because the main aim of our study is a qualitative analysis and an outline of the physical effects associated with phase dislocations rather than the exact quantitative results. For the same reason and to avoid long computer calculations, we have also chosen not as high an accuracy of simulations.

There are three critical parameters that significantly affect the final results: a grid step, a grid size, and the number of phase screens to be used in simulation. We have estimated these parameters with the following procedure. First the statistical quantity of interest is calculated with some initial magnitudes of the parameters. Then the same statistical quantity is recalculated with the decreased grid step and the increased grid size whereas the screen number remains the same. Varying the transverse grid parameters is continued until the difference between two successive estimations becomes no greater than 15%. Then the same procedure is repeated with the screen number. As a result, we arrived at the following transverse grid parameters: 512×512 grid size, $d = 0.1l_0$ grid step. Although it turned out that 20 phase screens are sufficient, a greater number of screens are used to get more points along the propagation path in some graphs below. The corresponding screen numbers are given in the figure captions.

The procedure of the simulations is as follows. First we generate a random sampling of the refractive-index field corresponding to the spectrum given by Eq. (30). Then a numerical solution of Eq. (29) with this refractive-index field is performed for a given propagation length L. As a result we get a sampling of complex field E at the aperture transverse to the propagation direction. Furthermore, the amplitude and the phase samples are extracted from the complex field sampling. These samples are used in the search of phase dislocations, which is

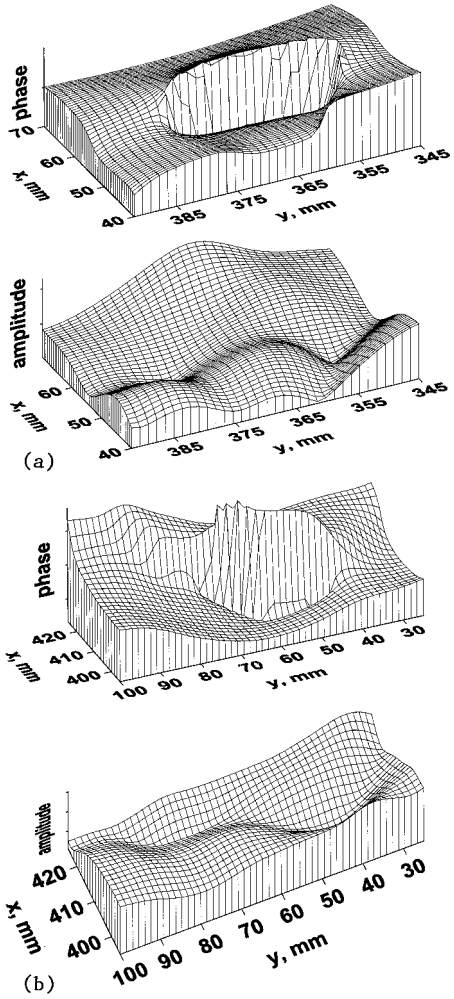

Fig. 3. Examples of phase dislocations obtained from simulations.

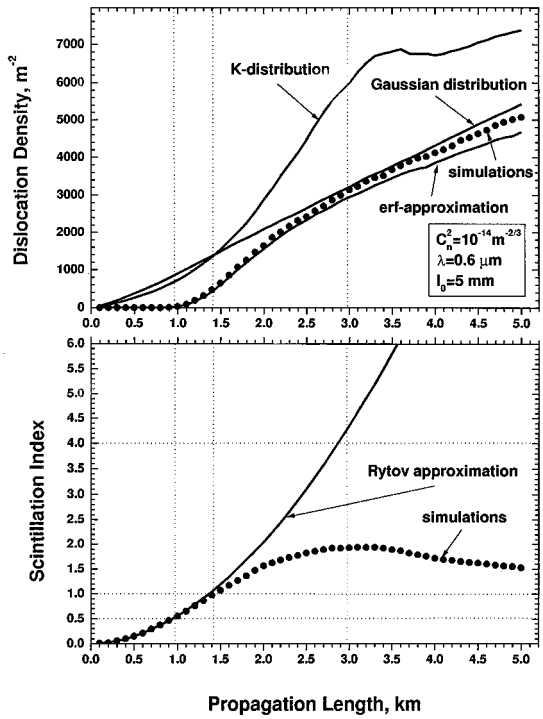

Fig. 4. Dislocation density (top graph) and scintillation index (bottom graph) versus propagation length. Fifty phase screens were used.

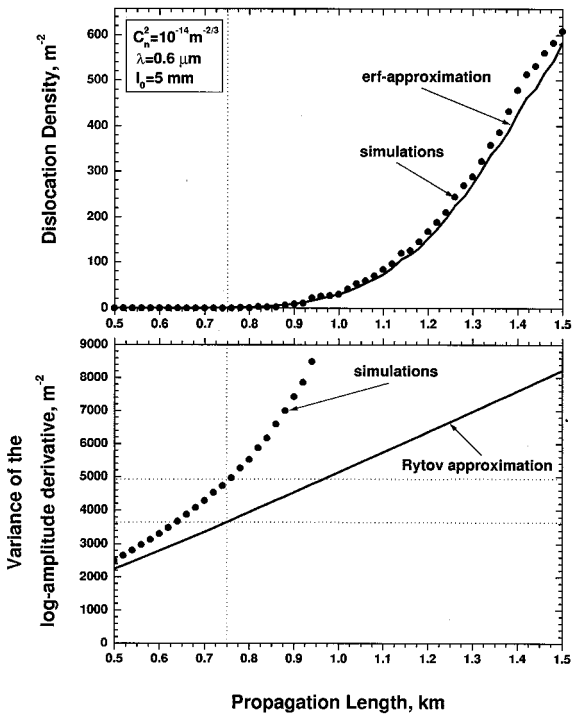

Fig. 5. Dislocation density (top graph) and variance of log-amplitude derivative (bottom graph) versus propagation length. The region of rapid growth of the density is shown. Seventy-five phase screens were used.

performed in two steps. In the first step the amplitude sampling is scanned to get the coordinates of all the points at which the amplitude has local minima. As a result we get a set of all suspicious points in which the phase vortices can appear, which allows us to narrow the area of future searching. Then these points are mapped onto the phase sampling and a phase tracing is performed around each of them. A vortex is considered to be found if the corresponding tracing reveals the $\pm 2\pi$ phase jump. The vortices with the $+2\pi$ (-2π) jump are considered as positive (negative) ones. An elective dislocation density is calculated for each sampling as half of the number of vortices divided by the area of the searching zone. These elective densities are averaged over all the samples to get the dislocation density, which is denoted in the graphs below as simulations. The variances $\sigma_{\chi_x}{}^2$ and $\sigma_{A_x}{}^2$ needed for the estimation of the dislocation density with the theoretical expressions [Eqs. (20), (25), and (28)] and the magnitude of the scintillation index β^2 are also calculated from the simulated samples, but the corresponding averaging is performed both inside each sampling and over all the samples.

Figures 3(a) and 3(b) show two examples of the phase dislocations that have been found in the sampling obtained under the following conditions: $C_n{}^2 = 10^{-14}\ \mathrm{m}^{-2/3}$, the wavelength $\lambda = 0.6\ \mu\mathrm{m}$, the inner scale $l_0 = 0.5$ mm, and the propagation length $L = 1.2$ km. In both figures the top graphs illustrate the dislocated phase surface whereas the graphs at the bottom present the corresponding amplitude. The points of zero amplitude responsible for the creation of the corresponding dislocations are clearly seen in the amplitude graphs.

The six graphs below show a behavior of the dislocation density for different turbulence and propagation conditions. In all the graphs we use the following notation. A direct count of the dislocation density from simulated samples is denoted as simulations and is plotted by filled circles. The theoretical predictions made with Eqs. (20), (25), and (28) are plotted by solid curves. We recall that the variances $\sigma_{\chi_x}{}^2$ and $\sigma_{A_x}{}^2$ that appeared in these equations are also obtained from simulated samples. The prediction by means of Eq. (20) is denoted as Gaussian distribution, the results obtained with Eq. (25) are denoted as K distribution, and the results following from Eq. (28) are denoted as erf approximation. In the bottom graphs of Figs. 4–7 we also compare the simulated scintillation index (Figs. 4 and 6) and the variance of log-amplitude derivative (Figs. 5 and 7) with the ones calculated in the Rytov approximation. In these graphs the simulated magnitudes and the theoretical results following from the Rytov solution are plotted by filled circles and by solid curves, respectively.

Figure 4 (top) plots the dislocation density versus the propagation length for given turbulence conditions. Below we distinguish four regions with different behaviors of the dislocation density that depend on the turbulence conditions. The boundaries of regions are indicated by thin dotted lines. For the quantitative estimations of the turbulence

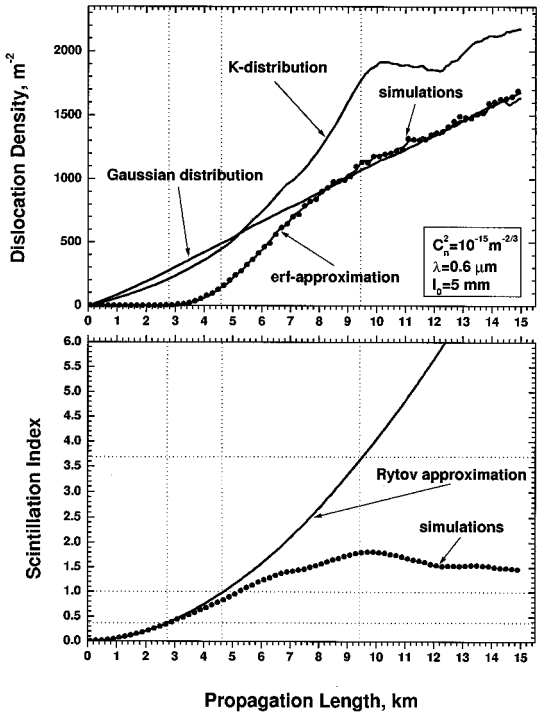

Fig. 6. Dislocation density (top graph) and scintillation index (bottom graph) versus propagation length. 150 phase screens were used.

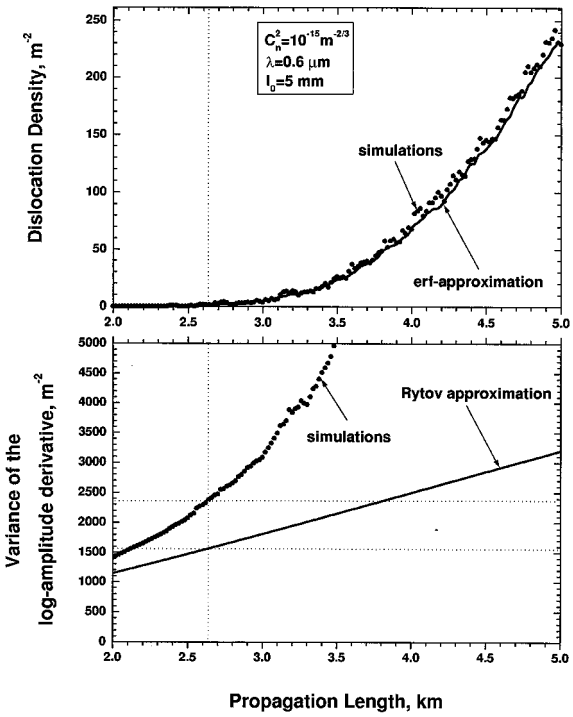

Fig. 7. Dislocation density (top graph) and variance of log-amplitude derivative (bottom graph) versus propagation length. The region of rapid growth of the density is shown. 250 phase screens were used.

conditions, the magnitude of scintillation index β^2 is commonly used. We estimate β^2 from the simulated data and calculate its Rytov approximation, ${\beta_R}^2$, by Eq. (15). Both quantities are plotted in the bottom graph for comparison.

The first one is a region of weak turbulence where the dislocations were not detected. However, we believe that the dislocations can occur inside this region but they were not detected because of the finite grid size and the sampling number. So we consider that in this region the dislocation density may be quite low but not exactly equal to zero. The corresponding magnitude of the scintillation index calculated in the Rytov approximation is inside the range ${\beta_R}^2 \lesssim 0.5$.

The second one is an intermediate region between the weak and the strong turbulences. The boundaries of this region may be approximately related with ${\beta_R}^2$ as $0.5 \lesssim {\beta_R}^2 \lesssim 1$. As one can see from the bottom graph, the upper boundary may also be considered as the conditions under which the Rytov approximation for the scintillation index starts to fall down. The dislocation density begins to grow rapidly at the outset of this region. Figure 5 (top) shows this effect in more detail. In the bottom graph of Fig. 5 we compare the simulated variance of the log-amplitude derivative with its Rytov approximation. As one can see by comparing the two graphs in Fig. 5, the lower boundary of this region may be related to the conditions under which the Rytov prediction for variance of the log-amplitude derivative differs strongly from the simulated data. We also note an interesting effect when dealing with the Rytov approximation. By comparing the bottom graphs in Figs. 5 and 6, one can see that the Rytov approximation for the variance of the log-amplitude derivative falls down well before that for the scintillation index. This effect is due mainly to the multiple scattering because it affects more strongly the log-amplitude derivative than it does the scintillation index. However, the Rytov approximation handles only partially the multiple scattering that leads to this effect.

In the third region ($1 \lesssim {\beta_R}^2 \lesssim 4$) the rapid growth of the dislocation density is replaced by a slower but still nonlinear increase. The upper-region boundary can be associated with the conditions under which the simulated scintillation index β^2 reaches the maximum.

In the fourth region, where the simulated scintillation index β^2 starts to saturate, the dislocation density grows almost linearly. Here both its functional behavior and its magnitude are close to the theory prediction for fully developed Gaussian fields. In our opinion, the small disagreement is due to the finite grid step: A number of small-sized dislocations that cannot be detected increase and start to be nonnegligible.

One can see the same salient features as above in Figs. 6 and 7, which have the same results as those given in Figs. 4 and 5, but for ten times weaker turbulence strength ${C_n}^2$.

Figure 8 presents the dislocation density versus wavelength. A decrease of density with wavelength can be explained as follows. The main reason for the dislocation appearance is a multiple scattering of light waves on the atmospheric inhomogeneities.

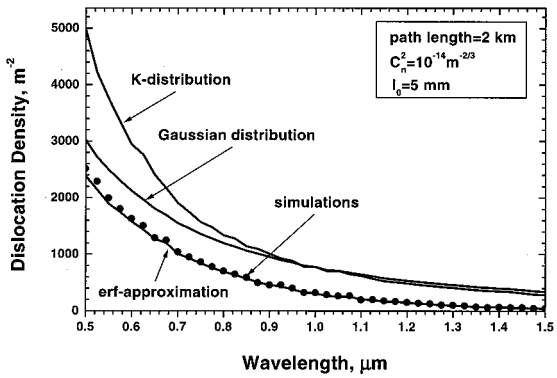

Fig. 8. Dislocation density versus wavelength. Twenty-five phase screens were used.

This effect becomes weaker as the wavelength increases, leading to a decrease of dislocation density.

Figure 9 shows the dislocation density as a function of the inner scale of turbulence. Similar to the wavelength dependence, the dislocation density decreases with the increase of the inner scale. The physics behind this effect is simple enough. As was mentioned in Section 4, small turbulence eddies make the main contribution to dislocation density. On the other hand, the size of these eddies is associated with the inner-scale magnitude. So the dislocation density grows as the inner scale decreases.

The results above allow for the following conclusions. The dislocation density depends strongly on the turbulence and the propagation conditions. Under very weak-turbulence conditions this quantity seems to be very low. Then, inside some intermediate region between the weak and the strong turbulences, it starts to grow rapidly, reaching quite quickly a magnitude of the order of 10^3 m^{-2}. Furthermore, under strong-turbulence conditions, this rapid growth is replaced by a slower but still nonlinear increase. And finally, under strong-turbulence conditions, the dislocation density increases almost linearly. In this case the simulated dislocation density is in good agreement with theoretical prediction for fully developed Gaussian fields. Unfortunately, neither this prediction, nor the one with the K distribution, allows for a satisfactory description under other turbulence conditions (as for the K distribution, it may be due to the rough approximation mentioned in Section 4).

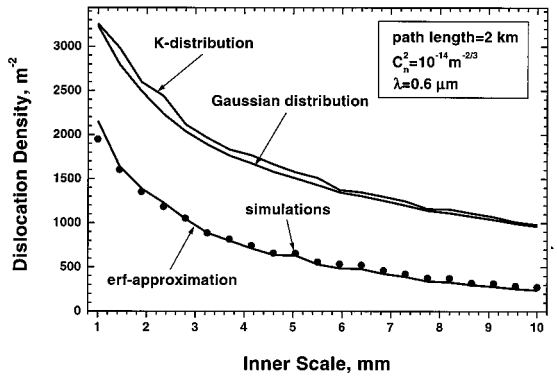

Fig. 9. Dislocation density versus inner scale of the turbulence. Twenty-five phase screens were used.

The comparison of simulated data with the empirical formula in Eq. (28) shows its applicability for a wide range of turbulent and propagation conditions. The predictions with this expression are in good agreement with the data for main dependences of interest, such as the dependence of the dislocation density on the turbulence strength C_n^2, on the propagation length, on the wavelength, and on the inner scale as well. So we can conclude that the empirical formula in Eq. (28) allows for a suitable description of the dislocation density.

6. Conclusions

The problem of turbulence-induced phase dislocations has been considered. The relatively simple expression for associated dislocation density involving only the PDF of a log-amplitude derivative has been derived. Based on this expression, the theoretical formulas that allow one to estimate the dislocation density for various turbulence conditions have been obtained. We have suggested an empirical formula for the density of interest that seems to be suitable for a wide range of turbulence and propagation conditions. The theoretical conclusions have been supported by the simulations by means of the numerical solution of a parabolic equation. The results obtained have allowed us to distinguish four interesting regions of turbulence conditions within which a different behavior of the dislocation density takes place. The first is a region in which the log-amplitude statistics are near Gaussian. This region can be associated with the very weak turbulence conditions, and the density of interest seems to be very low inside this region. The second is an intermediate region between the weak and the strong turbulences, where the dislocation density starts to grow rapidly. In the third region associated with the strong turbulence, the rapid growth of dislocation density is replaced by a slower but still nonlinear increase. And inside the final, fourth region where the turbulence can be considered as saturated, the dislocation density increases practically linearly in accordance with the theory prediction for fully developed Gaussian fields. The comparison of simulated data with the empirical formula allows for the conclusion that it provides a good continuous approximation of the dislocation density for various conditions.

The results obtained may have some promising applications in atmospheric optics. Among them, experimental investigations of turbulence-induced dislocations may be of help to estimate the upper boundary of the region where the Gaussian statistics are applicable for the log-amplitude fluctuations. The criterion of dislocation occurrence can also be used in theoretical research. For example, it may be useful to narrow the search area of a new strong-turbulence PDF of amplitude fluctuations. However, along with the usefulness of dislocations in

atmospheric optics, they could be potentially dangerous for adaptive optics and speckle interferometry. This conclusion was drawn by Fried and Vaughn[17] and supported later by Lukin and Fortes.[18] As for adaptive optics, both conventional measurements and conventional correction of a dislocated phase can give an unexpected result. The resulting quality of the correction depends on the size of the area covered by phase vortices. In connection with this, a spatial distribution of vortices is also of interest. A statistical treatment of this problem needs some additional investigation; below we discuss only some preliminary conclusions following from the visual observations of simulated samples.

In our opinion, a quite interesting effect takes place near the lower boundary of the region where the vortices just begin to occur in some detectable quantities. They do not appear completely independently inside the samples. Instead, several vortices group together, forming cobweblike fringes. The area occupied by these fringes is small compared with the sampling area. Then, with an increase in the magnitude of fluctuations, the number of fringes grows and the vortices start to cover empty places. Finally, when the turbulence conditions become strong enough, the vortices cover uniformly the whole sampling area.

The authors would greatly appreciate any experimental data on atmospherically induced phase dislocations.

This research was supported by Concejo Nacional de Ciencia y Tecnologia (Mexico) project 1020P-E9507 and by Sistema Nacional de Investigadores (Mexico). The authors are also grateful to the computer departments of Centro de Instrumentos and Direccion General de Servicios de Computo Academico (Universidad Nacional Autonoma de Mexico).

References

1. J. F. Nye and M. V. Berry, "Dislocations in wave trains," Proc. R. Soc. London Ser. A **336,** 165–190 (1974).
2. M. V. Berry, "Disruption of wavefront: statistics of dislocations in incoherent Gaussian random waves," J. Phys. A **11,** 27–37 (1978).
3. N. B. Baranova, B. Ya. Zel'dovich, A. V. Mamaev, N. Pilipetskii, and V. V. Shkukov, "Dislocations of the wavefront of a speckle-inhomogeneous field (theory and experiment)," JETP Lett. **33,** 195–199 (1981).
4. N. B. Baranova and B. Ya. Zel'dovich, "Dislocations of the wave-front surface and zeros of the amplitude," Zh. Eksp. Teor. Fiz. **80,** 1789–1797 (1981).
5. N. B. Baranova, A. V. Mamaev, N. Pilipetskii, V. V. Shkukov, and B. Ya. Zel'dovich, "Wave-front dislocations: topological limitations for adaptive systems with phase conjugation," J. Opt. Soc. Am. **73,** 525–528 (1983).
6. J. F. Nye, J. V. Hajnal, and J. H. Hannay, "Phase saddles and dislocations in two-dimensional waves such as tides," Proc. R. Soc. London Ser. A **417,** 7–20 (1988).
7. F. T. Arecchi, G. Giacomelli, P. L. Ramazza, and S. Residori, "Vortices and defect statistics in two-dimensional optical chaos," Phys. Rev. Lett. **67,** 3749–3752 (1991).
8. I. Freund and N. Shvartsman, "Wave-field phase singularities: the sign principle," Phys. Rev. A **50,** 5164–5172 (1994).
9. N. Shvartsman and I. Freund, "Vortices in random wave fields: nearest neighbor anticorrelations," Phys. Rev. Lett. **72,** 1008–1011 (1994).
10. I. Freund, "Optical vortices in Gaussian random wave fields: statistical probability densities," J. Opt. Soc. Am. A **11,** 1644–1652 (1994).
11. I. Freund and N. Shvartsman, "Structural correlations in Gaussian random wave fields," Phys. Rev. E **51,** 3770–3773 (1995).
12. I. Freund, "Saddles, singularities, and extrema in random fields," Phys. Rev. E **52,** 2348–2360 (1995).
13. I. Freund, "Amplitude topological singularities in random electromagnetic wavefields," Phys. Lett. A **198,** 139–144 (1995).
14. N. R. Heckenberg, M. Vaupel, J. T. Malos, and C. O. Weiss, "Optical-vortex pair creation and annichilation and helical astigmatism of a nonplanar ring resonator," Phys. Rev. A **54,** 2369–2378 (1996).
15. E. Abramochkin and V. Volostnikov, "Spiral-type beams: optical and quantum aspects," Opt. Commun. **125,** 302–323 (1996).
16. I. Freund, "Vortex derivatives," Opt. Commun. **137,** 118–126 (1997).
17. D. L. Fried and J. L. Vaughn, "Branch cuts in the phase function," Appl. Opt. **31,** 2865–2882 (1992).
18. V. Lukin and B. Fortes, "The influence of wave front dislocations on phase conjugation instability at thermal blooming compensation," Atmos. Oceanic Opt. **8,** 223–230 (1995).
19. V. A. Tartakovski and N. N. Mayer, "Phase dislocations and minimal phase representation of the wave function," Atmos. Oceanic Opt. **8,** 231–235 (1995).
20. B. V. Fortes and V. Lukin, "The effects of wavefront dislocations on the atmospheric adaptive optical systems performance," in Optics for Science and New Technology. Part II. Lasers and Laser Spectroscopy, J. Chang, J. Lee, and C. Nan, eds., Proc. SPIE **2778,** 1002–1003 (1996).
21. V. Aksenov, V. Banakh, and O. Tikhomirova, "Potential and vortex features of optical speckle fields," Atmos. Oceanic Opt. **9,** 1450–1456 (1996).
22. V. A. Tartakovski and N. N. Mayer, "Focal spot in the presence of phase dislocations," Atmos. Oceanic Opt. **9,** 1457–1460 (1996).
23. A. Ishimaru, *Wave Propagation and Scattering in Random Media* (Academic, New York, 1978), Vol. 2, Chap. 20.
24. A. Papoulis, *Probability, Random Variables, and Stochastic Processes* (McGraw-Hill, New York, 1984), Chap. 11.
25. V. I. Tatarski, *The Effects of the Turbulent Atmosphere on Wave Propagation*, NSF Report TT-68-50464 (U.S. National Science Foundation, Washington, D.C., 1968).
26. J. M. Martin and S. M. Flatte, "Intensity images and statistics from numerical simulation of wave propagation through 3-D random media," Appl. Opt. **27,** 2111–2126 (1988).
27. R. L. Fante, "Propagation of electromagnetic waves through turbulent plasma using transport theory," IEEE Trans. Antennas Propag. **AP-21,** 750–755 (1975).
28. G. Parry and P. N. Pusey, "*K* distribution in atmospheric propagation of laser light," J. Opt. Soc. Am. **69,** 796–798 (1979).
29. A. P. Prudnikov, Yu. A. Brychkov, and O. I. Marichev, *Integrals and Series* (Gordon & Breach, New York, 1990), Vol. 3, p. 40.